Variabilities observed in the vertical polarization electric field associated with electrojet current system during solar flare events

Gopika P G[1], Raj Kumar Choudhary[2], and Ambili K M[2]

[1]Space Physics Laboratory
[2]Vikram Sarabhai Space Centre

November 24, 2022

Abstract

Using ground based magnetometer data and an in-house developed quasi two dimensional (QTD) theoretical ionospheric model, we investigate differential response of the E region ionospheric current system to the solar flare events which occurred on 20 February 2002, and 24 September 2011. An abrupt increase in ΔH (positive crochet/Solar Flare Effect (SFE)) was observed at Thirunelveli during 24 September 2011 event, while a decrease in ΔH (reduced crochet/SFE) was observed during the other event. The reduction in ΔH was observed on 20 February when there were no signatures of counter electrojet (CEJ). As per QTD model simulations, the ratio of integrated Hall to Pedersen conductivity decreased more on 20 February at EEJ heights. As the conductivity ratio is directly proportional to the vertical polarization field, a decrease in conductivity leads to a reduced EEJ strength on 20 February 2002. In the presence of an additional SFE current system at the boundary between D and E region, during solar flare, the crochet is the resultant of EEJ and SFE. On 24 September, both the EEJ and SFE current systems were strong with the vortex center close to the equator and a positive crochet was observed. On 20 February, on the other hand, both EEJ and SFE were weak as the current vortex was away from the magnetic equator. Hence we surmise that SFE not only depends on the strength of the solar flare or the background electrojet condition but also the position of vortex of current systems.

Variabilities observed in the vertical polarization electric field associated with electrojet current system during solar flare events

P G Gopika[1], K M Ambili[1], R K Choudhary[1]

[1]Space Physics Laboratory, Vikram Sarabhai Space Centre, Thiruvananthapuram, Kerala India.

Key Points:

- Solar flare
- Integrated conductivity
- Quasi Two Dimensional Model

Corresponding author: K M Ambili, `ambili_km@vssc.gov.in, ambilisadasivan gmail.com`

Abstract

Using ground based magnetometer data and an in-house developed quasi two dimensional (QTD) theoretical ionospheric model, we investigate differential response of the E region ionospheric current system to the solar flare events which occurred on 20 February 2002, and 24 September 2011. An abrupt increase in ΔH (positive crochet/Solar Flare Effect (SFE)) was observed at Thirunelveli during 24 September 2011 event, while a decrease in ΔH (reduced crochet/SFE) was observed during the other event. The reduction in ΔH was observed on 20 February when there were no signatures of counter electrojet (CEJ). As per QTD model simulations, the ratio of integrated Hall to Pedersen conductivity decreased more on 20 February at EEJ heights. As the conductivity ratio is directly proportional to the vertical polarization field, a decrease in conductivity leads to a reduced EEJ strength on 20 February 2002. In the presence of an additional SFE current system at the boundary between D and E region, during solar flare, the crochet is the resultant of EEJ and SFE. On 24 September, both the EEJ and SFE current systems were strong with the vortex center close to the equator and a positive crochet was observed. On 20 February, on the other hand, both EEJ and SFE were weak as the current vortex was away from the magnetic equator. Hence we surmise that SFE not only depends on the strength of the solar flare or the background electrojet condition but also the position of vortex of current systems.

Plain Language Summary

Response of ionospheric current systems to solar flare events have been studied using magnetometer and an in-house developed ionospheric model. During an X1.9 class flare on 24 September 2011, the Equatorial Electrojet (EEJ) current was enhanced, where as during a M1.5 class flare on 20 February 2002, a depletion in EEJ was observed in magnetometer observations. During solar flare event, an additional current system (SFE) forms at the boundary between D and E region heights. The combined effect of EEJ and SFE current systems during solar flare events determines the flare response. Using model calculations we found that the integrated conductivity ratio controls the current density. On 24 September (equinox period) both EEJ and SFE current systems were near to equator and the effect of SFE was more evident leading to a positive crochet impact. On 20 February 2002 (winter equinox), on the other hand, SFE was far away from equator to show any impact. Hence during the first event, the effect of SFE is more visible in the magnetometer observations as an enhancement, where as during the second events SFE effect is minimum and EEJ is decreased in accordance with the decrease in the conductivity in the EEJ heights.

1 Introduction

Solar flares are sudden and intense brightenings of highly localized regions on the surface of the Sun. It is known that solar flares contribute as a main source of solar radiation in the EUV and X-ray wavelengths and thereby show a profound impact on the Earth's ionospheric system (Mitra, 2001; B. Tsurutani et al., 2005; B. T. Tsurutani et al., 2005; B. Tsurutani et al., 2009; Rao & Rao, 1963; Nagata, 1966; Oshio, 1967, references therein). The solar flare induced changes in the terrestrial ionosphere are generally referred to as "crochets" or Solar Flare Effects (SFE)(Campbell, 2003). The term crochet arises from a French word for hook because of its shape as seen on a magnetogram. It is now known also as solar flare effect (SFE) considering the location of its origin (Curto, 2020, references therein). the Crochets or SFEs, recorded by a magnetometer at ground, represent changes in the ionospheric currents associated with the arrival of enhanced electromagnetic radiations from the Sun (McNish, 1937a, 1937b; Rastogi, Rao, Alex, Pathan, & Sastry, 1997; Rastogi, Pathan, Rao, Sastry, & Sastri, 1999)

Near the magnetic dip equator, a belt of strong eastward current exists which extends to $\pm 3°$ latitude on the both sides of the dip equator and is termed as the Equatorial Electrojet (EEJ) current system. As the solar flare enhances the ionization and the conductivity, the EEJ current system in the ionosphere also get affected, and its signature gets imprinted in the ground based magnetometer observations as magnetic crochets (Rastogi et al., 1997, 1999; Chakrabarty, Bagiya, Thampi, Pathan, & Sekar, 2013; Xiong et al., 2014; Annadurai, Hamid, Yamazaki, & Yoshikawa, 2018). Many of the previous studies showed evidence for a concurrent enhancement in the EEJ during solar flares under normal electrojet conditions, which is known as positive crochet (Rastogi, 1996; Rastogi et al., 1999). Evidences are in plenty too to show negative SFEs during Counter Electrojet (CEJ) conditions with the further intensification of CEJ (Rangarajan & Rastogi, 1981; Rastogi et al., 1999). The intensification of CEJ by the solar flare is known as the negative solar flare effect or negative crochet and is suggested to be due to the counter electrojet currents at equatorial latitudes at the time of the flare (Rastogi, 1996).

Many studies reported that it is the pre-flare solar quite (Sq) current variations which controls the SFE in terms of the direction and magnitude (McNish, 1937b). The local time and latitude dependence of SFE amplitude were studied by Rangarajan and Rastogi (1981). They observed that SFEs were negative at the longitudes where morning counter electrojet prevailed. This implies that a same flare can cause different imprints on EEJ around the globe depending on the different pre flare ΔH conditions. Rastogi et al. (1997) reported changes in the three geomagnetic components H,Y and Z during a magnetic crochet on 15 June 1991 at different stations in the Indian sector. They reported a positive variation in H, a negative variation in Y and positive variation of Z near the magnetic equator.

Though it is typically observed that EEJ and CEJ strength get enhanced due to the enhanced E-region ionization associated with flares (Rastogi et al., 1999; Rastogi, Chandra, & Yumoto, 2013), some observations also suggest that flare related density enhancements at the magnetic equator can produce negative crochets even at the time of normal equatorial electrojet current/ Sq current (Curto, Amory-Mazaudier, Torta, & Menvielle, 1994a; Manju, 2016; Yamazaki, Yumoto, Yoshikawa, Watari, & Utada, 2009; Annadurai et al., 2018). Curto et al. (1994a) called this negative crochet as reversed SFE and reported that their occurrence is maximum during 10 – 12 LT. Hereinfater we will use the term reversed SFE for the negative crochet during normal EEJ/Sq period. Several explanations have been put forward for the occurrence of reversed SFE, but the exact reason is still unknown (Curto et al., 1994a; Curto, Amory-Mazaudier, Torta, & Menvielle, 1994b; Curto, 2020). Yamazaki et al. (2009) analyzed the reversed SFE which was confined to a limited longitude sector (around local noon) on 18 June 2000 and 3 July 2002. They conclude that reversed SFE at dip equatorial latitudes cannot be explained either by the morning or by the evening counter electrojet and its generation mechanism is not yet well understood. It was speculated that some local current systems (other than global Sq current system) might be responsible for the generation of reversed SFE.

Manju (2016) showed divergent responses of the vertical polarization electric field to the solar flares events on 9 September 2005 and 20 February 2002 using HF radar observations. An increase in the vertical polarization field was observed on 9 September, while it was shown to decrease during a M5.1 flare event on February 20, 2002. Recently Zhang, Liu, Le, and Chen (2017) studied the behavior of the equatorial electric field (EEF) measured by the Jicamarca Incoherent Scatter Radar(ISR) and JULIA system during solar flares between 1998 and 2008. The study revealed decrease in EEF and a negative correlation between the EEF and ΔH during solar flare events. They suggested that enhancement in the Cowling conductivity may modulate the ionospheric dynamo during solar flares. However, their observations were mainly restricted to the positive crochets of ΔH. Earlier Rastogi et al. (2013) had examined the existence of reversed SFE at dip equatorial stations during local noon time. They demonstrated that solar flares affect the electrojet current ($\sim$ 107 km) more than the global current (115 –120) as shorter wavelengths of the flare spectrum are generally absorbed in the lower regions of the ionosphere.

Another important study was the investigation of a differential response of ionosphere to the two solar flare events which occurred on 9 August 2011 and 24 September 2011 (Annadurai et al., 2018). A reduction of the eastward equatorial electrojet was observed during 9 August 2011 event, while the daytime eastward equatorial electrojet was seen to get enhanced during the 24 September 2011 event. Using spherical harmonic analysis of the observations from nearly 160 ground stations, Annadurai et al. (2018) showed that the equivalent current system of the geomagnetic crochets for the 24 September 2011 event had a similar behaviour as that of the background Sq current system, which, in turn, resulted in a positive crochet impact. On the other hand, the crochet current system revealed a different pattern compared to the background Sq current system on 9 August 2011. This study highlighted that crochet is not simply an enhancement of Sq but it a combined effect of background Sq and SFE current systems.

All these studies indicate that the impact of each solar flare on the EEJ can be different. This is perhaps because modulations in the ionospheric E-region conductivity and dynamo during reversed crochets is not fully understood. In this context, we studied the response of EEJ to two flares on 24 September 2011 and 20 February 2002. A X1.9 class of solar flare occurred on 24 September 2011 which started at 14:30 LT, peaked at 14:48 LT and ended at 15:00 LT. The other event was on 20 February 2002 when a M5.1 class of solar flare erupted at 11:00 LT, peaked at 11:20 LT, and ended at 11:24 LT. Both the flares peaked during local noon, but the solar flare on 24 September 2011 caused an enhancement in EEJ (positive crochet or SFE), whereas on February 20 2002, the normal EEJ was seen to get weakened (a reversed SFE) as a prompt response to the flare. Using an in-house developed quasi two dimensional physics based ionospheric model (QTD), we studied the response of the ionosphere to these two solar flare events and investigated the differences in the ionospheric conductivity in the lower and upper E region of the ionosphere. The observations and initial results are described in Section 2 followed by discussion and conclusion.

2 Observations

2.1 Background solar conditions

While extracting the solar flare impacts on the ionosphere, it is important to ensure that there were no geomagnetic storms and substorms during the period under study. The interplanetary electric field can cause prompt changes in the coupled magnetosphere-ionospheric system and mask all changes due to solar flare impact. Whenever there is a polarity reversal in the electric field, instantaneously get transmited and alter the ionosphere (Senior & Blanc, 1984). The interplanetary electric field, SymH index and auroral electrojet index on the two days (20 February 2002 and 24 September 2011) were examined (Figure not shown). During the flare period there were no changes of IMF polarity. On September 24, the maximum variation in SymH index was up to -10 nT while on February 20 it varied up to -15 nT. This shows that the effect of ring current on EEJ can be discounted. AE index was also checked to ensure that the auroral electrojet on September 24 and February 20 was also normal.

2.2 Solar flare events on 24 September 2011 and 20 February 2002

The solar X-ray flux of the two flares events were obtained from Geostationary Environmental Stationary Satellite (GOES) which provides the X-ray flux in the wavelength regime 0.1 –0.8 nm with 1 min cadence. The EUV fluxes were obtained from the Solar EUV Monitor (SEM) onboard SOHO satellite (Ogawa, McMullin, Judge, & Korde, 1993). The SEM experiment provides the EUV flux in two spectral bands (26 –34 nm and 0.1 –50 nm). We used 0.1 –50 nm spectral channel to study the impact of solar flares on the equatorial electrojet currents. The cadence of the EUV flux was 15 s.

On 24 September 2011, an X class flare (X1.9) erupted from the active region 1302 after the local noon. The temporal variation of X-ray and EUV flux are shown in Figure 1a. The flare started at 14:30 LT, peaked at 14:48 LT and ended at 15:00 LT. It was an impulsive flare which lasted for about 30 minutes. Compared to the pre-flare condition, the X-ray enhanced by a factor of 110 which is clear from the Figure 1a. The temporal variation of X-ray and EUV flux on 20 February 2002 is shown in Figure 1b. Three

M class flares occurred on this day at 7:54 LT, 11 LT and 15:06 LT respectively. The flares at 7:54 LT and 15:06 LT were M4.1 and M4.2 class flares respectively and that at 11:00 LT was a M5.1 class flare. On 20 February the flare started much early at 11:00 LT, peaked at 11:20 LT and ended at 11:24 LT. Compared to the X-class flare of September 24, the enhancement in X-ray on February 20 was about 60 times more than the pre-flare value.

As already discussed, previous studies have shown that the impact of each solar flares on the Earth's ionosphere is different. One factor which determines the effectiveness of solar flare is the Central Meridian Distance(CMD) from where the solar flare erupts. Depending on the CMD, a flare can be limb flare or central flare. A limb flare has a weaker impact on the ionosphere, compared to a central flare because the EUV fluxes, which are the main source of ionisation, would get absorbed by the solar atmosphere for a larger CMD of limb flare (Le, Liu, Chen, & Wan, 2013). In the present study, both flares were limb flares with CMD 59 and 66 respectively and hence EUV enhancement is very less compared to X-ray

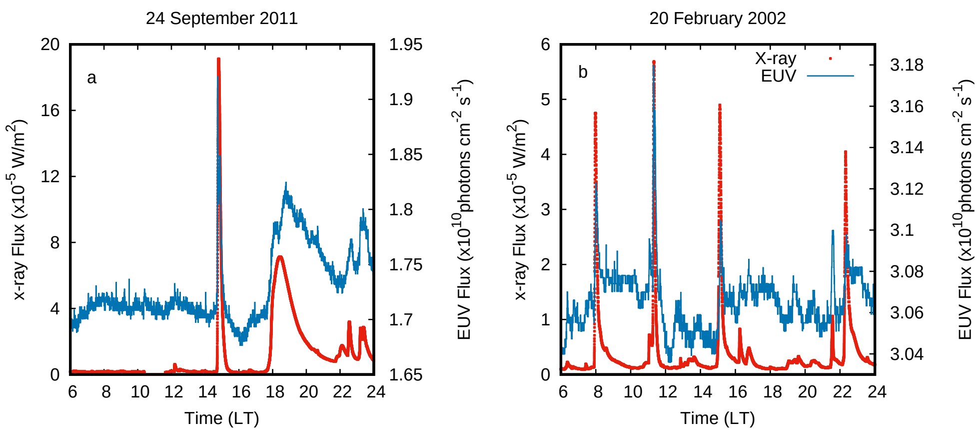

Figure 1. Temporal variation of X-ray and EUV flux a) on 24 September 2011 b) on 20 February 2002

2.3 Behaviour of the EEJ currents in response to solar flares

A magnetometer records the magnetic field fluctuations contributed by the local magnetic filed variations and global magnetic field fluctuations associated with ring currents (Rastogi & Klobuchar, 1990). To isolate the EEJ contributions from the total field, a method is to to subtract the ΔH values from a low latitude station like Alibagh from those at Tirunelveli (Nair, Rastogi, & Sarabhai, 1970; Rastogi & Klobuchar, 1990). But if the interest is to isolate the local magnetic field fluctuations from global one, the method proposed by Choudhary, St.-Maurice, Ambili, Sunda, and Pathan (2011) can be followed. The method is an empirical approach to assess how the global currents responsible for the SymH variations affected individual stations. We selected magnetometer observations (H^m_{SymH}) at Thirunelveli (8.71° N,77.75° E, dip-2.9°) in the local time interval 2 AM to 3 AM when local contributions are minimal. A linear regression is performed between H^m_{SymH} and Sym-H variations for the month during the local time interval 2 AM to 3 AM. This gave the average response of Thirunelveli for the month.

$$H^m_{SymH} = H_0 + C * SymH \tag{1}$$

where the background magnetic field H_0 and the constant C were obtained from a linear regression mentioned above. Hence the perturbation from local currents, ΔH can be obtained by removing the SymH contribution using the below equation

$$\Delta H = H_{obs} - H_0 - C * SymH \tag{2}$$

where H_{obs} is the observed magnetic field at any given time and Sym-H is the recorded value at the same particular time.

We have used the ground based magnetometer data provided by the Indian Institute of Geomagnetism, Mumbai to study the ΔH variation during solar flare events (`http://www.wdciig.res.in`). We chose these two flare events in our study as they are free from other space weather disturbances like Coronal Mass Ejections and associated geomagnetic disturbances and hece easy to isolate the effect of solar flare on ΔH. The conventional ground based magnetometer data with 1 min cadence is used in the study to understand the geomagnetic field variation during the solar flare.

Figure 2 a and b shows the comparison of ΔH observations on 24 September and 20 February with the nearest quiet day. As shown in Figure, the green line in figure corresponds to the ΔH value on flare day and the magenta line is for the quiet (control) day. The arrow indicates the time when the flare peaked. Figure2c and d are the enlarged portion of Figure 2 a and b. On 24 September, a positive crochet was observed during the peak phase of flare when ΔH increased by 18 nT (70%) compared to a quite day. The crochet was observed only on flare day and the ΔH recovered the control day value just after the flare. The arrow indicates the time when the flare peaked. We may note that with the commencement of the flare, ΔH showed a prompt enhancement and peaked with a time delay of 3 minute.

In Figure 2b, we can note how ΔH varied on February 20 2002. Since the first flare occurred during the morning hours, when the solar zenith angle was large, the ionization would be much low and any enhancement in ionization due to flare will not be reflected on ΔH. But surprisingly there is a prompt depression in ΔH from 130 nT to 110 nT and from 14 nT to 7 nT after the onset of flares at 11:00 LT and 15:06 LT respectively when we expected an enhancement due to enhanced conductivity during a solar flare. Despite the enhancement in the ionization, we observed a reduction in the horizontal magnetic field. Despite the fact that the flare occurred at normal electrojet time, a negative variation of SFE was observed at Thirunelveli on 20 February 2002. For this solar flare event, Manju (2016) had reported a decrease in vertical polarization electric field and the percentage of reduction in mean Doppler frequency was 15.6% at 106 km. Similarly the percentage of reduction observed in ΔH was 15.4%. We observed a ten minute time lag between the peak phase of flare and the maximum reduction in ΔH.

3 Model simulations by Quasi-two dimensional photochemical model

To understand reasons for the positive and negative effects of solar flare, the quasi two dimensional model (QTM) simulations are used. The QTM solves continuity equations using the method of characteristics for calculating ion and electron density (Ambili, St.-Maurice, & Choudhary, 2012; Ambili, Choudhary, St.-Maurice, & Chau, 2013). The model consider s photoionization, photo dissociative ionization, and photo electron impact ionization of four neutrals namely, NO, O_2, N_2 and O. It also includes photoionization of atomic oxygen (O) into metastable states such as $O^+(2D)$ and $O^+(2P)$. All chemical reactions including ion atom interchange reactions of atomic ions and subsequent dissociative recombination reactions of molecular ions are also included in the model (St-Maurice & Torr, 1978; Schunk & Nagy, 2000; Richards, 2011). The neutral density profiles of O_2, N_2 and O and the neutral temperature were obtained from Mass Spec-

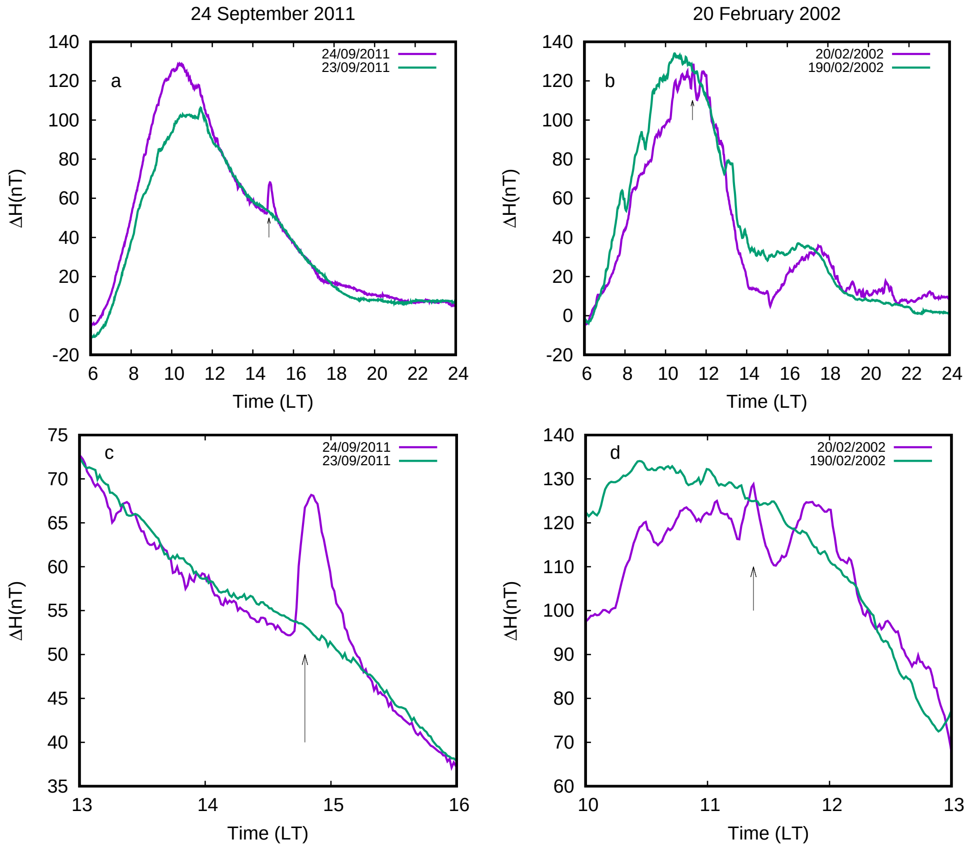

Figure 2. Temporal variation of a) ΔH over Thirunelveli 24 September 2011 b) ΔH over Trivandrum on 20 February 2002. Figures c and d are enlarged portions of a and b respectively

trometer Incoherent Scatter radar-E-90(MSIS-E-90) model `http://omniweb.gsfc.nasa.gov/vitm0/msis_vitmo.html`.The altitude profile of NO density is calculated in the model using the equations give by (Schunk & Nagy, 2000). IRI model gives the estimate of ion and electron temperature `http://ccmc.gsfc.nasa.gov/modelweb/models/iri_vitmo.php`. The SOLAR 2000 model is used to obtain the solar flux from 1 to 1350 Åwhich includes both X-ray and EUV fluxes. We have used the data from SOHO and GOES in the model also for reproducing the flare effect on solar flux during flare time. The relevant cross–sections and the resulting photoionization and photoabsorption rates were taken from references given in Schunk and Nagy (2000). More details on model is available in Ambili et al. (2012, 2013); Ambili, Choudhary, and St.-Maurice (2014).

To understand the flare impact on the D and E region of equatorial ionosphere, we only focus on the ionospheric region between 70 and 130 km which is a photochemistry dominated region and hence excluded the transport process. Since the time scale of the diffusion process is longer compared to the timescale of flare effect, we have omitted the diffusion process as well(Ambili et al., 2012). The model calculates the electron density at every 5 minute interval for an altitude range of 70-130 km at a vertical resolution of 1 km. The selected spatial and temporal resolution (1 km & 5 min) is sufficient to study the characteristics of ionosphere during solar flare events. To incorporate the enhancement in the solar flux during solar flare events, the entire wavelength regime (1 –1350 A) is multiplied by the enhancement factor obtained by GOES and SOHO data. The enhancement in both X-ray and EUV is obtained by dividing the flux by the preflare value of the flux, i.e, the flux before the onset of the flare. The electron density profile is simulated for two different conditions to compare how differently ionospheric traits appear when there is a solar flare and no solar flare. We simulated model runs for (a) non–flare case, without giving any enhancement in the solar radiation and (b) flare case which included the enhancement factor.

Figure 3a and b shows the electron density profiles for 24 September 2011 and 20 February 2002 cases simulated with QTD model during peak phase of flare. The red line in each figure shows the electron density profile for non–flare condition(i.e, without giving the flare enhancement factor in the radiation) and the black line represents the electron density with flare conditions. It is observed that during the pre-flare period, the density profiles simulated in the non–flare condition match well with the electron density profiles representing the flare condition. When the flare erupted, the density started increasing on both days and when the flares peaked, the density also peaked. On 24 September 2011, in the E region (above 90 km), the maximum electron density enhancement was 383% where the density increased from 8.87×10^4 cm^{-3} to 4.29×10^5 cm^{-3}. Below 90 km, in the D region, the electron density increased from 2.29×10^3 cm^{-3} to 2.24×10^4 cm^{-3} and the density enhancement was 880%. For the M class flare event on 20 February 2002, the maximum density enhancement is observed in the D region (615%) which had an increase from 4.71×10^3 cm^{-3} to 3.36×10^4 cm^{-3}. The E region was enhanced by 282% (from 1.18×10^5 cm^{-3} to 4.55×10^5 cm^{-3}). For both the flare cases, the D region density enhanced more compared to E region. Richmond and Venkateswaran (1971) showed that the X-rays in the 2 –10 Årange, which enhance during solar flares, are effective in ionizing the region at 80–100 km altitude (D region)

3.1 Variations in the Vertical polarization electric field during flare

The variations in the Equatorial electrojet current during solar flare event is associated with conductivity and electric field changes. The vertical polarization electric field (Ez) in the EEJ is given by the relation (Richmond, 1973)

$$Ez = \frac{\int \sigma_H ds}{\int \sigma_P ds} Ex \tag{3}$$

where Ex is the global curl free E-W electric field, σ_P is the Pedersen conductivity, σ_H is the Hall conductivity, and ds is the elemental length of the geomagnetic fileld line along which integration is carried out from an altitude in the dynamo region to an altitude, where the conductivities become negligibly small ($\sim$ 70 km). The Pedersen and Hall conductivities depend on the electron density (Ne), apart from collision and gyro frequencies of ions and electrons. The electron density (Ne) was estimated using QTD model for both the non-flare and flare conditions. The collision frequencies of the ions and electrons are calculated using the equations suggested by Schunk and Nagy (2000).

The conductivity is calculated using the collision frequency, electron density and gyro frequency of electrons and ions. The Pedersen (σ_P) and Hall(σ_H) conductivities are given as:

$$\sigma_P = N_e \times q_e \left(\frac{\nu_{in}}{m_i(\nu_{in}^2 + \omega_i^2)} + \frac{\nu_{en}}{m_e(\nu_{en}^2 + \omega_e^2)}\right) \tag{4}$$

$$\sigma_H = N_e \times q_e \left(\frac{\omega_e}{m_e(\nu_{en}^2 + \omega_e^2)} - \frac{\omega_i}{m_i(\nu_{in}^2 + \omega_i^2)}\right) \tag{5}$$

Here ω represents gyrofrequency of ions and electrons as indicated by the subscripts i and e, and ν represents the collision frequencies of ions with neutrals and electrons with neutrals as indicated by the subscripts in and en respectively. The integrated Hall and Pedersen conductivity ratios are calculated for flare and non-flare conditions.

Figures 3c and d respectively show the altitudinal variations in the ratio of the height integrated Hall and Pedersen conductivities on 24 September 2011 and 20 February 2002 at the peak phase of flares. The red line in the plots is the ratio of the conductivities that were calculated for non-flare ($r_{nonflare}$) while the black curve represents flare conditions (r_{flare}). As shown in the Figure, on 24 September 2011, the ratio decreased from 19.26

to 18.3 (5% reduction) in the E region, while it increased from 3.0 to 5.7, ie, 87% enhancement in the D region. On 20 February 2002 also the same features were observed but the percentage of deviation is -15% for the E (reduced from 18.7 to 15.7) and 52% (increased from 3.2 to 4.8) in the D region. It is very clear from the Figure that there is an altitude dependent variation in the conductivity ratio. The reason for the observed variation in integrated conductivity ratio directly related to the relative variation occurred in Pedersen and Hall conductivities as shown in Figure 3 e and f for the two flare cases.

It is clear from the Figure 3 that the Hall conductivity enhanced more than the Pedersen conductivityduring peak phase of flares around 90 km height. However the Pedersen conductivity is enhanced more in the EEJ height region (∼105 km). Hence the Hall to Pedersen conductivity ratio got enhanced in the D region and reduced in the E region. The percentage differences between the ratio for the flare and non flare cases ($\frac{r_{flare}-r_{nonflare}}{r_{nonflare}} * 100$) for the two flare cases are shown in Figure 4. During the quite period, when there is no flare, the difference is zero. But as the flare erupts, difference becomes positive in the D-region and increases as the peak phase of the flare approaches, and decays to zero when flare subsides. At the EEJ heights (above 105 km), on the other hand, the difference is negative and becomes minimum at the peak phase of the flare for both the flare cases. The difference is more positive (∼87%) in the D region on 24 September and more negative (15%) in the E region on 20 February. It is to be noted that variations in the height integrated conductivity depends not only on the magnitude of increase in electron density at different altitudes, but also on the shape of the electron density profile from D region and above (relative enhancement in each height), in addition to the time of occurrence of the flare (Manju & Viswanathan, 2005).

4 Discussion

It was earlier believed that the primary impact of a flare in the ionosphere was to increase the electron density, and hence crochets (SFEs) were considered just as an enhancement in the background Sq currents (McNish, 1937b). Later it was recognized that SFEs were actually due to an another current system, in addition to the normal Sq current system, forming during a solar flare (Van Sabben, 1961; Annadurai et al., 2018; Curto, 2020, reference therein). The enhanced conductivity in the D region or at the boundary between the D and E regions of the ionosphere (80 – 85 km) during flare is believed to cause the SFEs (Pinter, 1967). This current flows in the D region of the ionosphere with its foci away from that of the Sq current system (Curto et al., 1994a; Gaya-Piqué, Curto, Torta, & Chulliat, 2008; Van Sabben, 1961, 1968; Veldkamp & Van Sabben, 1960; Yasuhara & Maeda, 1961) which is located in the E-region of the ionosphere. A regular day to day variations in the geomagnetic field intensity on solar quiet days and EEJ over the geomagnetic equator controls the Sq current system between 90 and 120 km. Minor differences in the direction of the equivalent current between SFE and Sq/EEJ are attributed to the height difference of the current-flowing layer between SFE and Sq/EEJ (Van Sabben, 1961). We have studied the relative importance of the SFE and EEJ current system during a solar flare leading to varying signatures in the ground based magnetometers at the dip-equator. We used flare events on 24 September 2011 and 20 February 2002 for this study. A positive crochet impact was observed on 24 September 2011 and reversed crochet on 20 February 2002, while the flare happened around local noon time in both the cases with a normal EEJ during pre-flare period. The flare intensity however was different during the two events. While X-class flare was observed on 24 September 2011, the class of flare observed on 20 February was M1.

Over the geomagnetic equator, the EEJ is controlled by the vertical polarization electric field (E_z) which is directly correlated with the ratio of integrated Hall to Pedersen conductivity and the E-W zonal electric field, E_x (Ref. Equation 1). However since the E_x changes only slightly in the E region, it is the conductivity gradients which dominate the divergence of the vertical Hall current (Kelley, Ilma, & Crowley, 2009). During a solar flare event, huge enhancement in ionization, both in the D and E regions of the ionosphere, is observed associated with the EUV and X-ray outbursts of flares. The stronger solar flare has higher-energy (i.e., the shorter-wavelength) radiations which are generally absorbed at the lower regions of the ionosphere (D region). Richmond and Venkateswaran (1971) showed that the X-ray radiation in the 2 –10 Årange, which enhances during solar flares, are effective in ionizing the region around 80–100 km altitude. On 24 September, we observe that the D region plasma density got enhanced by 880%, while the enhancement in E region was 383% only. Even on 20 February, there was enhancement in D and E region plasma density during flare, albiet a less compared on 24 September. There were 615% and 282% density enhancements in D and E region respectively. We may also note that the flare not only enhanced the density, it also changed the shape of the profile and altered the integrated conductivity ratio as shown in Figure 3c and d and Figure 4. The conductivity ratio in the D region (below 90 km) enhanced by 52% on 20 February and 87% on 24 September. In the E region, on the other hand, this ratio decreased by 5% on 24 September, and 15% on 20 February.

Since changes in the conductivity ratio directly affects the strength of the vertical polarization electric field and hence the EEJ, it can be construed that the background vertical polarization electric field also got modulated by a factor as given by the percentage of deviation shown in Figure 4 during flare. We may therefore conclude that the current in the D region also might have been enhanced by ∼87% on 24 September and by ∼ 52% on 20 February. At the same time, the flare induced a reduction in vertical polarization electric field in the E region heights on both the flare cases with the percentage reduction more on 20 February (15%) than on 24 September (5%). The combined effect has been that though the flare induced a reduction in conductivity ratio at the E region on both the cases, a positive crochet was observed on 24 September and a negative crochet on 20 February.

A noteworthy part of observation on 20 February 2002 has been about 15% reduction in the ΔH over Trivandrum during the peak phase of the solar flare with a time delay of 10 minute. The HF radar at Trivandrum on 20 February had also noted a 15.6% decrease in the Doppler velocity at 106 km at the time of peak phase of the flare (Manju, 2016). As the HF radar observed Doppler velocity is directly proportional to the vertical polarization electric field, reduction in Doppler velocity stands for a decrease in the vertical polarization field and hence reduction is the EEJ. We calculated changes in conductivity ratio and hence the vertical polarization electric field (E_z) during flare using the QTD model, and with the help of Equation 1 found that the Ez also decreased by 15%. Thus even though the flare produced an enhancement in the D region conductivity ratio, the magnetometer observed a negative SFE impact. This result strongly suggests for the existence of factors other than a mere enhancement of solar radiation which modulate the appearance of the reversed SFE.

In a related study, Curto et al. (1994b) surmised that since the enhanced ionization during the flare time is at lower altitudes (below 100 km), there is a net descent in the "center of gravity" of the conducting mass. Using the neutral wind data obtained from the Saint-Santin radar, they showed that the horizontal wind below 100 km was eastward and wind reversed above 110 km. The descending motion of the conducting mass, combined with the direction of neutral winds in the lower and middle parts of the dynamo region produced a change in the direction of the integrated current. Hence at the lower altitudes, the currents were westward and above 110 km, where Sq current exists, the currents were eastward. Yamazaki et al. (2009) also suggested that the reverse SFE can be caused by the low-altitude westward currents enhanced during a solar flare. Here we did a similar analysis to see if there was a differential wind on 20 February 2002 which resulted in a negative crochet. Since we do not have real measurements of winds either on 20 February 2002 and 24 September 2011, we used horizontal wind model results (Hedin, 1992) to derive altitudinal variations in the neutral winds at Trivandrum. In Figure 5 we show the altitudinal profile of zonal winds on 24 September 2011 and 20 February 2002 respectively. We may note that there was no reversal in the direction of the neutral wind on either of the days below 110 km and the winds remained westward where both EEJ and SFE induced current systems exist. This suggests that the reversed SFE observed on 20 February 2002 may not be due to the westward current generated by eastward winds.

A time delay between the solar flare onset and negative crochet occurrence have been shown to be related to the time taken by equivalent SFE current to develop. Analyzing the 9 August 2011 solar flare event, Annadurai et al. (2018) suggested that the equivalent SFE current system, which represents the ionospheric current system superposed on the background Sq current system, shows response in about 3 minute after the occurrence of the solar flare. Our observation shows a time delay of 10 minute in the occurrence of a reversed crochet in response to solar flare. The exact reason for reversed crochet at noon time, in the absence of CEJ, however is not well understood.

The above discussions can be summarized as follows

1. The net effect of the solar flare at the equatorial ionosphere current system depends on the strength and positioning of the flare induced currents system (SFE), and the background solar quite current votex (Sq Current system). Van Sabben (1961) reported that the current system induced by SFE is not symmetrical about the geomagnetic equator and showed seasonal shift in vortex centre as shown by

solar daily variation. The Sq vortex centre is generally at a lower latitude than those of the SFEs. The mean difference in latitude is 6°. The positioning of these vortex centres is important in determining the strength of current systems at the equator. If the Sq current vortex is far away from the magnetic equator, as in the Winter solstice period, considerable reduction in EEJ is observed (St-Maurice, Ambili, & Choudhary, 2011; Yamazaki & Maute, 2017). Hence on 24 September, the strength of EEJ and SFE is more compared to 20 February.

2. In September, the background EEJ is already strong because daily variation vortex is near by the equator and the SFE current system is also strong during the equinox period Van Sabben (1961). Hence the decrease in the vertical polarization field (by 5%) at the EEJ height may not be as effective as the 87% enhancement in SFE current system in the magnetometer observations as a positive crochet (70% of enhancement in EEJ during the peak phase of flare). As discussed by Annadurai et al. (2018), the equivalent current system of the geomagnetic crochets (SFE) during the 24 September 2011 flare event also showed a similar pattern with the background Sq current system at low and mid latitudes and a positive crochet in magnetometer.
3. Manju (2016) explained the decrease in the vertical polarization electric field on February 20 2002, as observed by HF radar at Trivandrum, by replicating the electron density profiles in two different ways. First case: E-region was given 30 times enhancement but D region was increased only by 3 times with respect to the normal; second case: D region was increased by an order of 2 and E region by a factor of 2. These density profiles were then used to create the ratio of height integrated Hall to Pedersen conductivity. In the first case, the ratio of the integrated conductivity increased when there was flare but in the second case, when the enhancement was more in the D region, the ratio decreased at EEJ heights. We also followed the same method but instead of randomly enhancing the density, we calculated the electron density profile using the QTD model and incorporated the exact enhancement in the EUV and X-ray from SOHO and GOES respectively in the solar flux at the time of flare. For both flares, enhancements in the D region were more compared to E region. This is understandable because during flare, enhancement is more in X-ray compared to EUV and short wavelength (high energetic X-rays) can penetrate more to D region and cause enhanced ionization. In

fact, D region ionization is more when the flare is stronger. It is also worthwhile to note that both flare are limb flare and EVU enhancement might be minimum (Le et al., 2013) to enhance E region as reported by Manju (2016). Hence the relative enhancement of D and E region density as proposed by Manju (2016) might not be the reason for positive and reversed crochets during solar flares.

4. As the EEJ currents are weaker during winter solstice period (Yamazaki & Maute, 2017, references there in), any further reduction in vertical polarization field at the time of a flare can further reduce the strength of EEJ . We may note that the reduction in Doppler frequency as observed by HF radar (Manju, 2016), reduction in the vertical polarization electric field estimated using QTD model, and the reduction in ΔH strength observed by magnetometers were all $\sim$15%. It is clear from the above discussion that the effect of the SFE current system, which was enhanced during flare was minimum at the equator. This is because as reported by Van Sabben (1961); Curto et al. (1994a), the SFE vortex is at higher latitude than those of daily variation Sq, that means it is further away from the equator during the Winter solstice period. Hence the effect of the SFE current system is minimal. Referring to earlier flare studies, it is observed that compared to equinox and summer solstice, the magnitude of crochet is always small during the winter solstice period (Manju & Viswanathan, 2005; Chakrabarty et al., 2013).
5. Curto et al. (1994b) reported that the reversed SFE is a combined effect of descending motion of enhanced conducting mass and the existence eastward winds at the lower altitudes. However the present analysis didn't show any indication of eastward winds and hence westward currents at the lower altitudes where SFE exists.
6. Yamazaki et al. (2009) reported that reversed SFE around noon time might be caused by the low-altitude westward currents enhanced by an intense solar flare. From our calculations, it is clear that the current system, produced by SFE at the lower altitude (D region), depends on the background condition. SFE can generate a westward current only if there is westward wind or a CEJ (partial CEJ) conditions prevails at the dip-equator (Rastogi et al., 1999, 2013). On the other hand, SFE can simply enhance the background current system without altering the direction. On 20 February 2002, there is no evidence of CEJ or partial CEJ, hence reversed SFE observed was not because of enhanced west ward current system.

It is related to the position of the SFE and Sq vortex centres and the strength of the two current systems.

From above discussion, it is clear that the crochet which is present during solar flare is because of the current system which is developing during solar flare. The magnitude and direction of crochet not only depends on the enhancement of ionization, but also on the strength and position of back ground Sq/EEJ, and SFE current systems. Depending up on the position of Sq vortex, seasonal variations in EEJ strength is observed at equatorial region (Yamazaki & Maute, 2017). Positioning of Sq vortex center also affect the SFE vortex and its latitudianl shift (Van Sabben, 1961; Curto et al., 1994a, 1994b). Curto et al. (1994a) reported that at equinox, the SFE and Sq vortices happen to be at same latitudes. However, in summer a difference as high as of 11° is observed. During equinox period, when both EEJ and SFE are strong and close to equator we can expect a positive crochet. Negative crochet (enhancement of ΔH in the negative direction) is present only if CEJ/partial CEJ prevails in the E region. However reversed crochet is reduction in magnetic field during normal EEJ/Sq period. It is the resultant of Sq and SFE current systems. The crochet is determined by the relative strength of the two current systems at the equator. Curto et al. (1994a) reported that reversed SFE is the resultant of variations in the ionospheric current system geometry due to the displacement of the SFE system in longitude and/or latitude with respect to the Sq system. He also also proposed that negative SFE must appear in zones between the focus of the vortice.

Finally, a note on the seasonal and solar activity impact. A X-class flare event happened on September 24 2011, which is autumnal equinox period while the M5.1 class flare event happend on February 20 2002 which was the end of winter solstice period. Also, 2002 falls in the active phase of the solar cycle 23 while 2011 is the solar minimum period of the solar cycle 24. In order to evaluate how the flare intensity vis-a-vis solar activity and solar season impacts on the crochet formations, we made some hypothetical model runs for both the events. For September 24 2011, we reduced the Xray and EUV intensity to make the X-class flare intensity to a M class flare, and increased on February 20 2002 to make it an X-class flare. Though the intensity of the flares was changed, we could not observe any drastic change in the difference in the ratio of the integrated conductivities during the two events. This indeed indicates that the seasonal variation of current system also contributes to the observed phenomenon. This may be one of the reasons that reduced crochet is not common for all flares. Hence, the SFE not only depends on the strength of the solar flare or the background electrojet conditions, but also on the position of Sq and SFE vortex of current system and its seasonal and solar activity variation. More detailed and quantitative analysis is required to understand the occurrence of reduced SFE around noon time when normal EEJ prevails.

5 Conclusion

We studied the response of EEJ to two flare events on 24 September 2011 and 20 February 2002. A positive crochet was observed in the magnetometer observations on the first event, whereas a reduced crochet (negative crochet during a normal EEJ period) was observed on the second event. It is normal to observe a negative crochet in the presence of CEJ or partial CEJ. It was however interesting to note that on 20 February, there was no CEJ or partial CEJ signatures in ΔH at the time of flare when a negative crochet was observed. We investigated reasons for positive and reduced crochet using the QTD model simulations. The ratio of integrated Hall to Pedersen conductivity was calculated based on the model results. We observed that the ratio in the D region was enhanced during both the flare events while the ratio depleted in the E region with maximum depletion on 20 February. We analysed all the factors which might be affecting the strength and direction of crochet. It is known from the past studies that during solar flare an additional current system forms at D region or boundary between D and E region heights. Effectively there are two current systems during solar flare and the crochet is the resultant of the two current systems. The solar flare can enhance the ionization and conductivity and hence the strength of the current systems but do not alter their direction.

During equinox period, EEJ is strong with the vortex center close to the equator (Yamazaki & Maute, 2017). As reported in the earlier studies, during equinox period SFE current system is also close to the Equator (Van Sabben, 1961; Curto et al., 1994a). Since SFE current vortex is close to the equator, we can expect the maximum effect during equinox period. Hence on 24 September, even though the conductivity ratio was decreased by 5% at EEJ heights ($\sim$ 105 km), a positive crochet was observed. Actually this enhancement in magnetic field is the contribution from D region current system. Since EEJ is relatively strong, the decrease in conductivity ratio at EEJ height is not affected much. However on 20 February, EEJ itself is weak as the current vortex is $\sim$35° away from the magnetic equator. According to Van Sabben (1961), the SFE current vortex might be further pole ward. Hence the effect of SFE is minimum and its not visible in the magnetometer observations. However, 15% reduction observed in Δ H directly correlated to the 15% reduction in the integrated conductivity ratio at the EEJ heights. Hence we concluded that SFE not only depends on the strength of the solar flare or the background electrojet condition but also the position of Sq and SFE vortex of current system and its seasonal and solar activity variation.

Acknowledgments

This work is supported by Department of Space, Government of India and INSPIRE research project, Department of Science and Technology, Government of India. The authors gratefully acknowledges GOES (`https://www.ngdc.noaa.gov/stp/satellite/goes/dataaccess.html`) and SOHO team (`https://dornsifecms.usc.edu/space-sciences-center/download-sem-data/`)for X-ray flux and EUV intensity data sets used in the study. The ground based magnetometer data over Trivandrum and Alibag were obtained from Indian Institute of Geomagnetism, Mumbai (`http://www.wdciig.res.in`). Thanks are due to the WDC-C2 (Kyoto) for the auroral electrojet and geomagnetic indices data.

References

Ambili, K., Choudhary, R., & St.-Maurice, J.-P. (2014). Seasonal differences in the sunrise undulations at the dip equator at solar minimum at two distinct locations and their relation with postsunset electrodynamics. *Journal of Geophysical Research: Space Physics*, *119*(7), 5777–5789.

Ambili, K., Choudhary, R., St.-Maurice, J.-P., & Chau, J. L. (2013). Nighttime vertical plasma drifts and the occurrence of sunrise undulation at the dip equator: A study using jicamarca incoherent backscatter radar measurements. *Geophysical Research Letters*, *40*(21), 5570–5575.

Ambili, K., St.-Maurice, J.-P., & Choudhary, R. (2012). On the sunrise oscillation of the f region in the equatorial ionosphere. *Geophysical research letters*, *39*(16).

Annadurai, N. M. N., Hamid, N. S. A., Yamazaki, Y., & Yoshikawa, A. (2018). Investigation of unusual solar flare effect on the global ionospheric current system. *American Jeophysical Union*. doi: 10.1029/2018JA025601

Campbell, W. H. (2003). *Introduction to geomagnetic fields.* Cambridge University Press.

Chakrabarty, D., Bagiya, M. S., Thampi, S. V., Pathan, B., & Sekar, R. (2013). Signatures of moderate (m-class) and low (c and b class) intensity solar flares on the equatorial electrojet current: Case studies. *Journal of Atmospheric and Solar-Terrestrial Physics*, *105*, 170–180.

Choudhary, R. K., St.-Maurice, J. P., Ambili, K. M., Sunda, S., & Pathan, B. M. (2011). The impact of the January 15, 2010, annular solar eclipse on the equatorial and low latitude ionospheric densities. *J. Geophys. Res.*, *116*. doi: 10.1029/2011JA016504

Curto, J. J. (2020). Geomagnetic solar flare effects: a review. *Journal of Space Weather and Space Climate*, *10*, 27.

Curto, J.-J., Amory-Mazaudier, C., Torta, J., & Menvielle, M. (1994a). Solar flare effects at ebre: Regular and reversed solar flare effects, statistical analysis (1953 to 1985), a global case study and a model of elliptical ionospheric currents. *Journal of Geophysical Research: Space Physics*, *99*(A3), 3945–3954.

Curto, J.-J., Amory-Mazaudier, C., Torta, J., & Menvielle, M. (1994b). Solar flare effects at ebre: unidimensional physical, integrated model. *Journal of Geophysical Research: Space Physics*, *99*(A12), 23289–23296.

Gaya-Piqué, L., Curto, J., Torta, J., & Chulliat, A. (2008). Equivalent ionospheric currents for the 5 december 2006 solar flare effect determined from spherical cap harmonic analysis. *Journal of Geophysical Research: Space Physics*, *113*(A7).

Hedin, A. (1992). Horizontal wind model (hwm)(1990). *Planetary and Space Science*, *40*(4), 556–557.

Kelley, M. C., Ilma, R. R., & Crowley, G. (2009, May). On the origin of pre-reversal enhancement of the zonal equatorial electric field. *Annales Geophysicae*, *27*, 2053 - 2056. doi: 10.5194/angeo-27-2053-2009

Le, H., Liu, L., Chen, Y., & Wan, W. (2013). Statistical analysis of ionospheric responses to solar flares in the solar cycle 23. *Journal of Geophysical Research: Space Physics*, *118*(1), 576–582.

Manju, G. (2016). On the unique divergent response of the equatorial electrojet vertical polarization electric field to different solar flare event. *Journal of Geo-*

physical Research Space Physics, *121*. doi: 10.1002/2015JA021588

Manju, G., & Viswanathan, K. S. (2005). Response of the equatorial electrojet to solarflare related x-ray flux enhancements. *Earth Planets Space*, *57*.

McNish, A. (1937a). Magnetic effects associated with bright solar eruptions and radio fade-outs. *Nature*, *139*(3510), 244–244.

McNish, A. (1937b). Terrestrial-magnetic and ionospheric effects associated with bright chromospheric eruptions. *Terrestrial Magnetism and Atmospheric Electricity*, *42*(2), 109–122.

Mitra, A. P. (2001). Ionospheric e ects of solar flares. *Journal of Atmospheric and Solar-Terrestrial Physics*.

Nagata, T. (1966). Solar flare effect on the geomagnetic variation. *Journal of geomagnetism and geoelectricity*, *18*. doi: 10.5636/0021-9169(61)90164-7

Nair, K. N., Rastogi, R. G., & Sarabhai, V. (1970, May). Daily Variation of the Geomagnetic Field at the Dip Equator. *Nature*, *226*, 740 - 741. doi: 10.1038/226740a0

Ogawa, H. S., McMullin, D. R., Judge, D. L., & Korde, R. S. (1993). Normal incidence spectrophotometer with high-density transmission grating technology and high-efficiency silicon photodiodes for absolute solar extreme-ultraviolet irradiance measuremen. *Optical Engineering*, *32*(12), 3121–3126.

Oshio, M. (1967). Solar flare effects on geomagnetic field. *Rep. Ionos. Space Res. Japan*, *21*, 77–114.

Pinter, S. (1967). Geomagnetic crochets of solar flares observed in hurbanovo. *Bulletin of the Astronomical Institutes of Czechoslovakia*, *18*, 274.

Rangarajan, G. K., & Rastogi, R. G. (1981). Solar flare effect in equatorial magnetic field during morning counter electrojet. *Indian Journal of Radio and Space Physics*, *10*.

Rao, K. R., & Rao, M. P. (1963). On the location of the ionospheric current system causing geomagnetic solar flare effects. *Journal of the Atmospheric Sciences*, *20*(6), 498–501.

Rastogi, R. G. (1996). Solar flare effects on zonal and meridional currents at the equatorial electrojet station, annamalainagar. *Journal of Atmospheric and Terrestrial Physics*, *58*.

Rastogi, R. G., Chandra, H., & Yumoto, K. (2013). Unique examples of solar flare effects in geomagnetic h field during partial counter electrojet along cpmn longitude sector. *Earth Planet Science*, *65*. doi: 10.5047/eps.2013.04.004

Rastogi, R. G., & Klobuchar, J. A. (1990). Ionospheric electron content within the equatorial F2 layer anomaly belt. *J. Geophys. Res.*, *95*, 19045.

Rastogi, R. G., Pathan, B. M., Rao, D. R. K., Sastry, T. S., & Sastri, J. H. (1999). Solar flare effects on the geomagnetic elements during normal and counter electrojet periods. *Earth Planets Space*, *51*.

Rastogi, R. G., Rao, D. R. K., Alex, S., Pathan, B. M., & Sastry, T. S. (1997). An intense sfe and ssc event in geomagnetic h , y and z fields at the indian chain of observatories. *Ann Geophysical Research Letters*, *15*. Retrieved from http://www.ann-geophys.net/15/1301/1997 doi: 10.1029/2004GL021475,2005a.

Richards, P. G. (2011). Reexamination of ionospheric photochemistry. *J. Geophys. Res.*, *116*, A08307. doi: 10.1029/2011JA016613

Richmond, A. (1973). Equatorial electrojeti. development of a model including winds and instabilities. *Journal of Atmospheric and Terrestrial physics*, *35*(6), 1083–1103.

Richmond, A., & Venkateswaran, S. (1971). Geomagnetic crochets and associated ionospheric current systems. *Radio Science*, *6*(2), 139–164.

Schunk, R. W., & Nagy, A. F. (2000). *Ionospheres: Physics, Plasma Physics, and Chemistry.* (Vol. 59). Cambridge: Cambridge University Press.

Senior, C., & Blanc, M. (1984). On the Control of Magnetospheric Convection by the Spatial Distribution of Ionospheric Conductivities. *J. Geophys. Res.*, *89*(A1), 261 - 284. doi: 10.1029/JA089iA01p00261.

St-Maurice, J.-P., Ambili, K. M., & Choudhary, R. K. (2011). Local electrodynamics of a solar eclipse at the magnetic equator in the early afternoon hours. *Geophys. Res. Lett.*, *38*, L04102. doi: 2010GL046085

St-Maurice, J. P., & Torr, D. G. (1978). Nonthermal rate coefcients in the ionosphere : The reactions of o + with n2 , o2 , and no. *Journal of Geophysical Research*.

Tsurutani, B., Judge, D. L., Guarnieri, F. L., Gangopadhyay, P., Jones, A. R., Nuttall, J., ... Viereck, R. (2005). The october 28, 2003 extreme euv solar flare and resultant extreme ionospheric effects: Comparison to other halloween events and the bastille day event. *Geophysical Research Letters*, *32*. doi: 10.1029/2004GL021475,2005a.

Tsurutani, B., Verkhoglyadova, O., Mannucci, A., Lakhina, G., Li, G., & Zank, G. (2009). A brief review of solar flare effects on the ionosphere. *Radio Science*. doi: 10.1029/2008RS004029

Tsurutani, B. T., Judge, D. L., Guarnieri, F. L., Gangopadhyay, P., Jones, A. R., Nuttall, J., … Viereck, R. (2005). The october 28, 2003 extreme euv solar flare and resultant extreme ionospheric effects: Comparison to other halloween events and the bastille day event. *Geophysical Research Letters*, *32*. doi: 10.1029/2004GL021475,2005a.

Van Sabben, D. (1961). Ionospheric current systems of ten igy-solar flare effects. *Journal of Atmospheric and Terrestrial Physics*, *22*.

Van Sabben, D. (1968). Solar flare effects and simultaneous magnetic daily variation, 1959–1961. *Journal of Atmospheric and Terrestrial Physics*, *30*(9), 1641–1648.

Veldkamp, J., & Van Sabben, D. (1960). On the current system of solar-flare effects. *Journal of Atmospheric and Terrestrial Physics*, *18*(2-3), 192–202.

Xiong, B., Wan, W., Zhao, B., Yu, Y., Wei, Y., Ren, Z., & Liu, J. (2014). Response of the american equatorial and low-latitude ionosphere to the x1.5 solar flare on 13 september 2005. *Journal of Geophysical Research Space Physics*, *121*. doi: 10.1002/2015JA021588

Yamazaki, Y., & Maute, A. (2017). Sq and eeja review on the daily variation of the geomagnetic field caused by ionospheric dynamo currents. *Space Science Reviews*, *206*(1-4), 299–405.

Yamazaki, Y., Yumoto, K., Yoshikawa, A., Watari, S., & Utada, H. (2009). Characteristics of counter-sq sfe (sfe*) at the dip equator cpmn stations. *Journal of Geophysical Research*, *114*. doi: 10/1029/2009JA014124

Yasuhara, M., & Maeda, H. (1961). Geomagnetic crochet of 15 november 1960. *Journal of Atmospheric and Terrestrial Physics*, *21*(4), 289–293.

Zhang, R., Liu, L., Le, H., & Chen, Y. (2017). Equatorial ionospheric electrodynamics during solar flares. *Geophysical Research Letters*, *44*(10), 4558–4565.

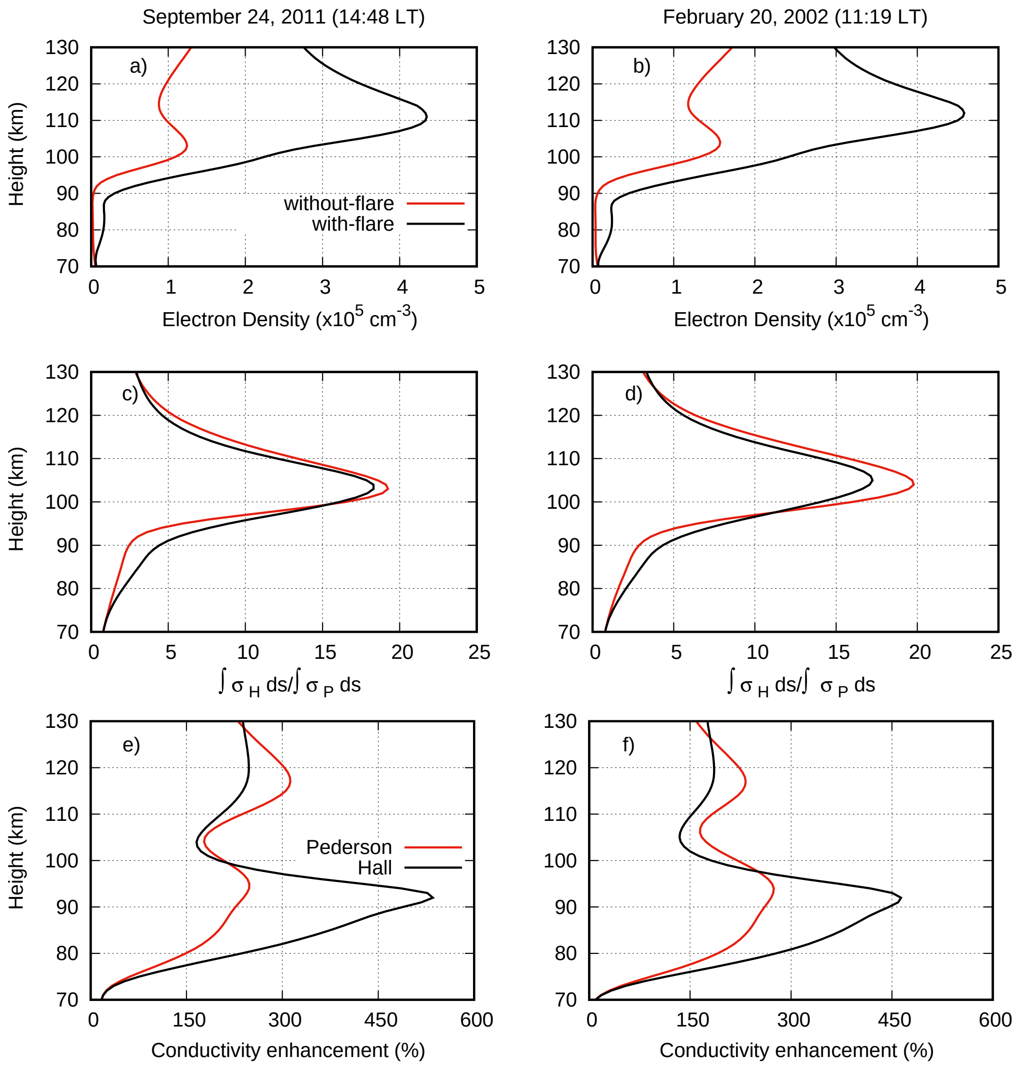

Figure 3. Altitude variation of a) Electron density during flare and non flare period on 24 September 2011 b) Same as that of Panel a on 20 February 2002 c) Integrated conductivity ratio during flare and non flare period on 24 September 2011 d) Same as that of Panel c on 20 February 2002 e) Enhancement in Pedersoan and Hall conductiity on 24 September 2011 d) Same as that of Panel e for 20 February 2002

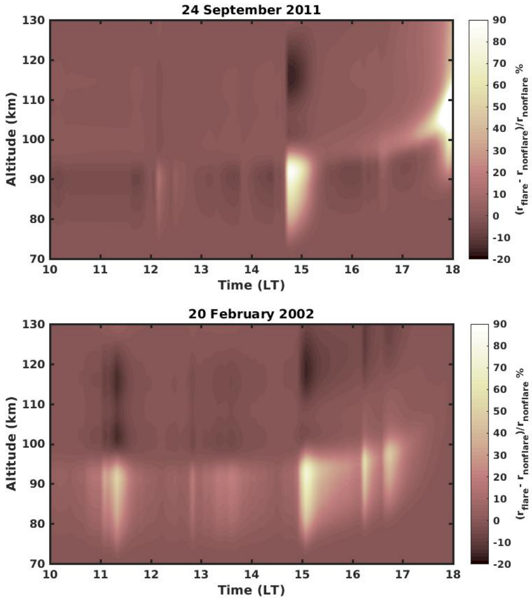

Figure 4. Temporal variation of percentage of deviation of integrated conductivity ratio a) on 24 September 2011 b) on 20 February 2002

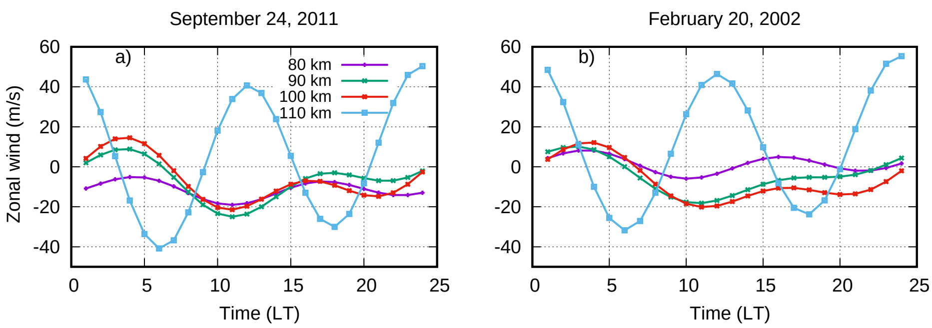

Figure 5. Temporal variation of zonal wind at various altitudes at a) on 24 September 2011 b) on 20 February 2002